

# Hybrid-Segmentor: A Hybrid Approach to Automated Fine-Grained Crack Segmentation in Civil Infrastructure

June Moh Goo<sup>a,\*</sup>, Xenios Milidonis<sup>b</sup>, Alessandro Artusi<sup>b</sup>, Jan Boehm<sup>a</sup>, Carlo Ciliberto<sup>c</sup>

<sup>a</sup>*Department of Civil, Environmental and Geomatic Engineering, University College London, Gower Street, London, WC1E 6BT, United Kingdom*

<sup>b</sup>*DeepCamera MRG, CYENS Centre of Excellence, Nicosia, Cyprus*

<sup>c</sup>*Department of Computer Science, University College London, Gower Street, London, WC1E 6BT, United Kingdom*

---

## Abstract

Detecting and segmenting cracks in infrastructure, such as roads and buildings, is crucial for safety and cost-effective maintenance. In spite of the potential of deep learning, there are challenges in achieving precise results and handling diverse crack types. With the proposed dataset and model, we aim to enhance crack detection and infrastructure maintenance. We introduce Hybrid-Segmentor, an encoder-decoder based approach that is capable of extracting both fine-grained local and global crack features. This allows the model to improve its generalization capabilities in distinguish various type of shapes, surfaces and sizes of cracks. To keep the computational performances low for practical purposes, while maintaining the high the generalization capabilities of the model, we incorporate a self-attention model at the encoder level, while reducing the complexity of the decoder component. The proposed model outperforms existing benchmark models across 5 quantitative metrics (accuracy 0.971, precision 0.804, recall 0.744, F1-score 0.770, and IoU score 0.630), achieving state-of-the-art status.

*Keywords:* Deep Learning Applications, Semantic Segmentation, Convolutional Neural Networks, Transformers, Hybrid Approach, Crack

---

\*

*Email address:* `june.goo.21@uc1.ac.uk` (June Moh Goo)

## 1. Introduction

Cracks in roads, pavements, and buildings pose a serious threat to public safety, causing accidents and damage to vehicles on roads and pavements, and influencing public safety and financial burden on buildings. Traditionally, manual inspections have been used to identify cracks in civil infrastructure, but these methods are labor-intensive, subjective, and prone to human error, resulting in inconsistent results and potential disasters. Therefore, automated crack detection is necessary to provide an objective and highly accurate alternative. Machine learning methods, such as deep learning models, can be used to detect, segment, or classify damage to civil infrastructure, which can be facilitated by the widespread deployment of surveillance and traffic-monitoring cameras. However, training accurate models for crack segmentation is challenging due to a scarcity of well-annotated and diverse datasets, which impacts model robustness and generalizability. Our research aims to address this crucial data gap and develop automated crack detection to prevent dangers and reduce financial risks to communities. Progress in this direction could lead to real-time identification of cracks in the future, ensuring a more dependable and safe utilization of critical concrete structures.

The main contributions of this work are:

- Combine and refine publicly available crack datasets to create an enhanced and comprehensive crack segmentation dataset.
- Introduce a data refinement methodology to combine publicly available datasets using image processing techniques.
- Introduce the Hybrid-Segmentor model to efficiently detect cracks in infrastructures, which is based on the encoder-decoder architecture that convolutional neural networks (CNNs) and transformers have efficiently used in the past.
- Emphasize the remarkable ability of the proposed model to perform effectively across a diverse range of surface types and under challenging imaging conditions, such as blurred images and areas with complex crack contours.

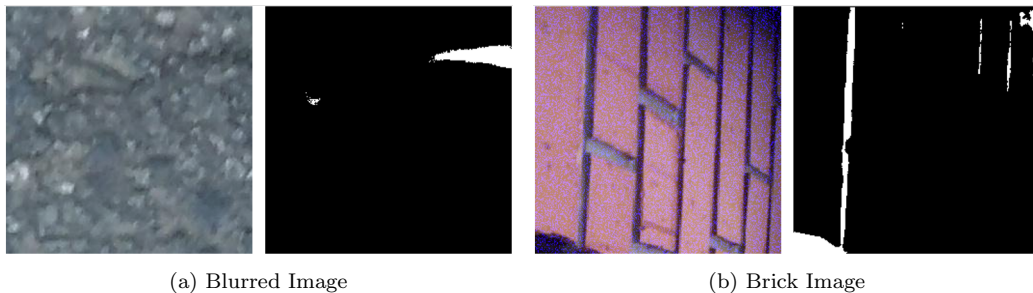


Figure 1: Representative failures in crack detection by traditional models: (a) shows a prediction by a Fully Convolutional Network (FCN) on a blurred image, incorrectly marked as a crack, highlighting difficulties with image clarity. (b), from a U-Net architecture, displays a brick pattern where the borders of the bricks are wrongly identified as cracks, revealing challenges in differentiating structural boundaries

- The code, trained weights of the model, and the full dataset for experiments are publicly available and can be accessed here:  
<https://github.com/junegoo94/Hybrid-Segmentor>

## 2. Related Work

One of the earliest methods for crack detection was a CNN-based model for pixel-level crack detection using FCN [1]. This approach achieves end-to-end crack detection, significantly reducing training time compared to CrackNet [2], a CNN-based model that was the State-Of-The-Art (SOTA) in 2017 without using a pooling layer. While thin cracks can be accurately predicted across a variety of scenes, further enhancements are needed to capture real-time level predictions. In a similar aspect, DeepCrack [3] improves on the generalization of FCN architecture by incorporating batch normalization and side networks for faster convergence. Additionally, this research proposes the publicly available DeepCrack dataset [3], which enhances crack detection precision across diverse scenes. Cheng et al. propose a full crack segmentation model based on U-Net [4]. Subsequent research further demonstrated that the U-Net is particularly suited for crack segmentation tasks [4, 5, 6, 7, 8]. Some researchers pinpoint that using classical image classification structures as encoders, pre-trained with data such as ImageNet [9], strengthens feature extraction in crack segmentation networks, enhancing crack detection performance [6].

In addition, various encoder-decoder models have been introduced in the

field. Amongst these, DeepCrack2 (not to be confused with ‘DeepCrack’ in [3] bearing the same name; we refer to this model as ‘DeepCrack2’ from this point onwards to avoid confusion) is a deep convolutional neural network designed to facilitate automated crack detection through end-to-end training [10]. It primarily focuses on acquiring high-level features that effectively represent cracks. This approach involves the integration of multi-scale deep convolutional features obtained from hierarchical convolutional stages. This fusion enables the capture of intricate line structures, with finer-grained objects in larger-scale feature maps and more holistic representations in smaller-scale feature maps. DeepCrack2 adopts an encoder-decoder architecture similar to SegNet [11] and employs pairwise feature fusion between the encoder and decoder networks at corresponding scales. DeepCrack2 is one of the most benchmarked models in the crack segmentation community.

Despite the abundance of studies that either employ existing deep learning models or enhance them, these approaches may not always result in effective or efficient results in real-world scenarios (Fig.1). Recently, HrSegNet [12] was proposed as an approach to consistently maintain high resolution in the images, distinguishing itself from methods that restore high-resolution features from low-resolution ones. Furthermore, the model enhances contextual information by leveraging low-resolution semantic features to guide the reconstruction of high-resolution features [12]. These features helped HrSegNet-B64 reach SOTA accuracy and inference speed in crack segmentation.

### 3. Dataset

We introduce a large refined dataset with the aim of creating a significantly larger and more diverse resource for crack segmentation compared to what is currently available in literature. Since the existing datasets contain a relatively small number of images compared to other well-known tasks in computer vision, large-scale deep learning models are at a high risk of overfitting in these settings. In contrast to most datasets for crack segmentation that collect data based on a single type of surface, the refined comprehensive dataset includes a wide range of surfaces to enhance the robustness and generalizability of trained models. Additionally, due to the characteristics of some cracks, each existing image has a small proportion of crack pixels, which could result in a form of class imbalance. To counteract this bias,

we employed a data augmentation strategy to increase the number of crack pixels in our dataset.

### 3.1. Sub-Dataset Details

We identified 13 open-source datasets that include different surfaces of pavements, walls, stone, and bricks. Table 1 shows the details of each dataset. Some datasets provide samples either collected with specific acquisition systems and under diverse background settings (e.g. Aigle-RN, ESAR, and LCMS that collectively form the AEL Dataset) [13]; or acquired with smartphone cameras (e.g. CRACK500) [14]. A number of small datasets provide road and pavements images, including CrackTree260, CRKWH100, CrackLS315 and Stone331 [15]. (e.g. CrackTree260 is a dataset of 260 visible-light road pavement images constructed based on the CrackTree206 [16]) DeepCrack [3] is a large dataset created as a publicly available benchmark dataset consisting of crack images captured across various scales and scenes, specifically designed to evaluate the performance of crack detection systems. The German Asphalt Pavement Distress (GAPs) dataset, introduced in [17], addresses the comparability issue in pavement distress research, offering a standardised dataset with 1,969 high-quality gray valued images. It covers various distress classes, including cracks, potholes, and inlaid patches. The images have a resolution of  $1,920 \times 1,080$  pixels with a per-pixel resolution of  $1.2 \text{ mm} \times 1.2 \text{ mm}$ . To enable pixel-wise crack prediction, 384 images are manually selected from GAPs and annotated, forming the GAPs384 dataset [18]. Masonry is created consisting of images captured from masonry structures, which exhibit intricate backgrounds and a diverse range of crack types and sizes [19]. CrackForest dataset (CFD), one of the most benchmarked datasets, is a labeled collection of road crack images, designed to represent the typical conditions of urban road surfaces [20, 21]. Finally, SDNET2018 is a dataset comprising more than 56,000 images of cracked and non-cracked concrete bridge decks, walls, and pavements, with crack widths ranging from 0.06 mm to 25 mm. Since the dataset does not contain ground truth masks, we use this dataset only for the collection of non-cracked image data [22].

### 3.2. Data Refinement

Ground truth masks in existing datasets were generated using different methods, leading to varying resolutions, distortions, and discontinuity. To address this inconsistency, masks were manually inspected and refined using basic image processing where deemed necessary to ensure no irregularities

Table 1: Sub-datasets details before data refinement.

Dataset	Size	Resolution	Surface	Crack Proportion (%)
Aigle-RN	38	Various Sizes	Pavement	0.71
CFD	118	480 x 320	Pavement	1.62
CRACK500	500	2000 x 1500	Pavement	6.01
CrackLS315	315	512 x 512	Pavement	0.25
CrackTree260	260	Various Sizes	Pavement	0.46
CRKWH100	100	512 x 512	Pavement	0.36
DeepCrack	537	544 x 388	Diverse surfaces	3.5
ESAR	15	512 x 768	Pavement	0.6
GAPs384	384	640 x 540	Pavement	0.36
LCMS	5	1000 x 700	Pavement	0.67
Masonry	240	224 x 224	Bricks/Masonry walls	4.21
SDNET2018	56092	256 x 256	Pavement	-
Stone331	331	512 x 512	Stone Surfaces	0.11
Total Dataset				2.69

were present, based on a process described previously [23]. Due to the inconsistency of AEL datasets with the rest of the datasets (inverted and not binary), dedicated processing steps were performed. First, the values in the masks were inverted. Pixels were then converted to either black or white based on a threshold of  $255/2$ . All images included in our dataset were then cropped to  $256 \times 256$  resolution without overlapping. Finally, due to the reduced number of images with cracks, we augmented our dataset with a significant portion of cracks to address class imbalance. Specifically, images with masks containing over 5000 crack pixels were selected for augmentation, where Gaussian noise was added, and a random rotation of  $90^\circ$ ,  $180^\circ$ , or  $270^\circ$  was applied. Non-crack data from the SDNet2018 dataset [22] were also added. Fig. 2 shows how the original ground truth improved after the refinement process. Irregularities such as small holes, discontinuity, and thinness were corrected. Furthermore, adding the augmented dataset increased the proportion of the crack pixels by 5.8%, which aims to mitigate class imbalance problems. As a result, we created a comprehensive refined dataset with a total of 12,000 images, which is the largest crack dataset to the best of our knowledge.

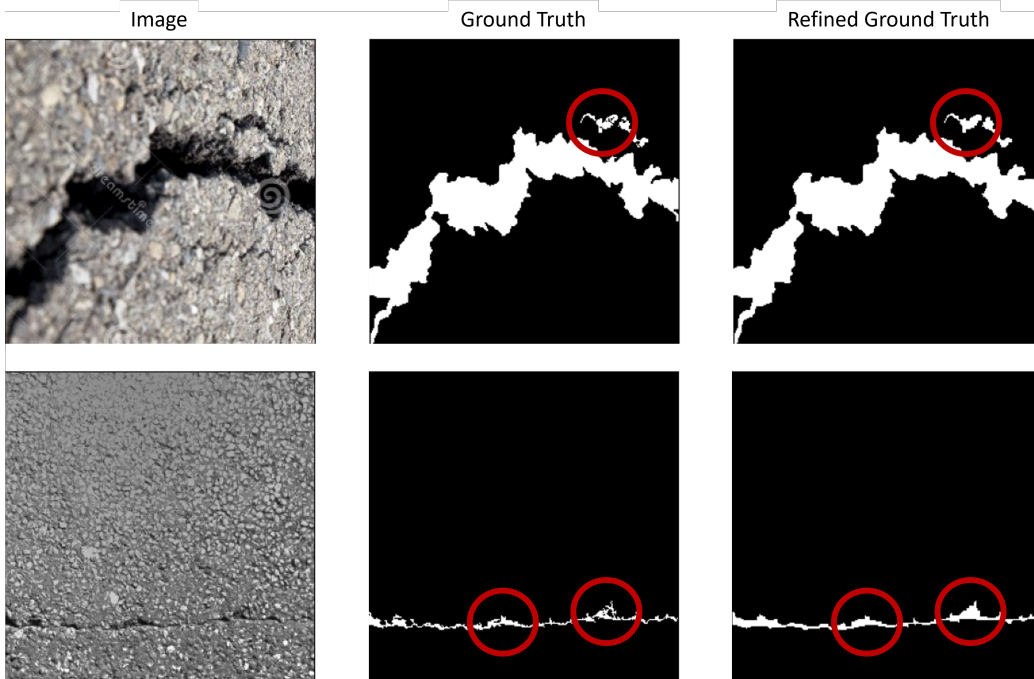


Figure 2: The figure shows the improvement in small holes, discontinuity and thinness of the ground truth after applying appropriate image processing methods.

#### 4. Model Design

This section provides an in-depth overview of our Hybrid-Segmentor, an end-to-end crack segmentation model. As illustrated in Fig. 3, the input images to our model are going through two distinct encoders: the CNN (ResNet-50 [24]) and the Transformers (SegFormer [25]) paths. Each of these encoders generates 5 multi-scale feature maps, which are then fused together at each of the 5 intermediate stages. In the last step, the fused feature maps are utilized to produce the final output (simplified decoder). The overall benefits of our Hybrid-Segmentor, through the combination of the two different deep learning architectures are the ability to detect local details and global structural understanding, while spatial hierarchy leads to more accurate crack detection. Integrating features at different scales from both paths enables effective recognition of cracks of various sizes and shapes, leveraging the strengths of both local and global analysis. This ensures higher accuracy and robustness in detecting cracks in diverse types of surfaces. Sections 4.1 and 4.2 further describe the benefits introduced by the CNN and transformer

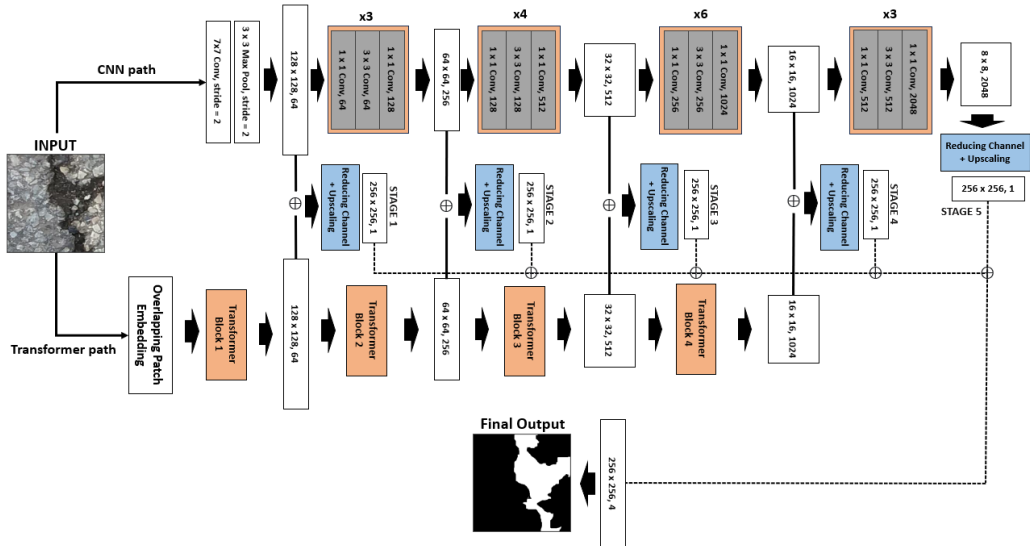


Figure 3: The Hybrid-Segmentor architecture: the upper path for CNN and the lower for Transformers. Each path generates feature maps at every layer, and the central blue boxes represent the concatenation of these feature maps.

paths of our architecture respectively.

#### 4.1. CNN Path

The use of a CNN architecture is guided from the fact that we would like to capture local features from the input image. These features are both fine-grained local details, e.g., small cracks or textures, and high level features, such as abstract shapes. This is achieved through the spatial hierarchy property of the ResNet-50 model used in our Hybrid-Segmentor, which allows the detection of various image features at multiple scales. Additionally, its translation invariant property will help with extracting features regardless of the crack position within the input image. Finally, its capability to preserve high-resolution details will make our model more effective at detecting small cracks or local variations.

#### 4.2. Transformer Path

The use of a transformer in crack segmentation aims to extract global features from the input image, which are crucial for capturing the overall shape and appearance of a crack. Here, we use as our base key concepts from the SegFormer model [25]. Through its self-attention mechanism, this



model can recognise the continuity and structure of cracks that span distant regions, understanding how different parts of the crack relate to each other across the image (Long-range Dependency Capture). SegFormer also incorporates a spatial hierarchy, similar to CNNs, by processing features at different scales, making it able to capture both fine details and global structures. Another important property of the SegFormer is its global consistency, which by analysing the image entirely, it provides insights into how cracks are distributed across the entire image, ensuring a coherent understanding of the crack patterns.

The transformer of our proposed model utilizes three additional key concepts, which are explained below: Overlapping Patch Embedding 4.2.1, Efficient Self-Attention 4.2.2, and Mix-Feed Forward Network (FFN) 4.2.3.

#### 4.2.1. *Overlapping Patch Embedding*

Local continuity is crucial for preserving fine-grained details and spatial coherence, which is important for accurate semantic segmentation. The first iterations of vision transformers used non-overlapping patch embeddings, which could lead to a loss of local continuity between patches. However, to address this, we utilized overlapping patch embedding, as introduced by SegFormer [25], which better preserves local continuity.

The Vision Transformer (ViT) [26] is an innovative approach to computer vision. It treats images as sequences of patches and processes them similarly to how transformers handle sequences of words in natural language processing. In a typical ViT architecture, an image is divided into  $N \times N$  patches, which are then linearly embedded into  $1 \times 1 \times C$  vectors. While this method enables the model to effectively capture global context, it can still be challenging to maintain local continuity among patches when  $N \times N \times 3$  image patches are represented as  $1 \times 1 \times C$  vectors.

To address this issue, SegFormer employed Overlapping Patch Embedding. Instead of simply dividing the image into non-overlapping  $4 \times 4$  patches for vector embedding, Overlapping Patch Embedding takes inspiration from how CNNs use sliding windows with defined parameters such as kernel size (K), stride (S), and padding (P). It predefines these parameters to split the input image into patches of size  $B \times C \times K^2 \times N$ , where  $B$  represents the batch size,  $C$  is the number of channels times the stride squared, and  $N$  is the number of patches. Merging operations are then performed to transform the reshaped patches to  $B \times C \times W \times H$ , where  $W$  and  $H$  represent the width and height of the merged patches, respectively. As a result, the model captures

both fine-grained local details and broader global features more effectively, addressing the issue of losing local continuity while still maintaining global context.

#### 4.2.2. Efficient Self-Attention

Especially in models like SegFormer with smaller patch sizes like  $4 \times 4$ , the self-attention layer presents computational challenges. The traditional multi-head attention process involves creating matrices for query (Q), key (K), and value (V), all of which have dimensions  $N(H \times W) \times C$ , and performing computations using the scaled dot-product attention equation as shown in equation 1.

$$\text{Attention}(Q, K, V) = \text{Softmax}\left(\frac{QK^T}{\sqrt{d_{head}}}\right)V \quad (1)$$

When dealing with large input images, the computational complexity of the provided equation 1 can lead to a significant increase in model weight. Therefore, the method that reduces the  $N(H \times W)$  channels of  $K$  and  $V$  by applying a sequence reduction process based on a predefined reduction ratio is proposed [25]. It is possible to reshape the equation by dividing  $N$  by  $R$  and multiplying  $C$  by  $R$ .  $C \times R$  dimensions can be reduced to  $C$  dimensions by linear operation, resulting in  $\frac{N}{R} \times C$  dimensions for Key and Value matrices. Especially useful for tasks like semantic segmentation, this method efficiently manages computational complexity while preserving representation power (equation 2).

$$\begin{aligned} \hat{K} &= \text{Reshape}\left(\frac{N}{R}, C \cdot R\right)(K) \\ K &= \text{Linear}(C \cdot R, C)(\hat{K}) \end{aligned} \quad (2)$$

#### 4.2.3. Mix-FFN

ViT [26] uses positional encoding for local information, which comes with fixed input resolution constraints and suffers performance drops as resolution changes. In order to overcome this issue, researchers replace positional encoding with a Convolutional  $3 \times 3$  kernel in the FFN, asserting its non-essential role and providing flexibility without resolution restrictions.

$$\mathbf{x}_{out} = \text{MLP}\left(\text{GELU}\left(\text{Conv}_{3 \times 3}\left(\text{MLP}\left(\mathbf{x}_{in}\right)\right)\right)\right) + \mathbf{x}_{in} \quad (3)$$

In this regard, the equation 3 simply adds a Convolutional  $3 \times 3$  layer to the existing FFN within the Transformer encoder. By replacing traditional positional encoding with this adaptation, the model performance is maintained while fewer parameters are required.

### 4.3. Decoder

The CNN and transformer paths of our model result in substantial model complexity and size. In order to balance this, the decoder is designed to be as simple as possible. A  $256 \times 256 \times 1$  feature map is generated by concatenating the outputs from both paths, as shown in Fig. 3. Feature maps from each stage are combined to create a multi-scale, multi-layer feature map, which is then used to create the final output. By integrating the strengths of both paths, this approach optimizes performance and efficiency while simplifying the decoder.

## 5. Experimental Settings

### 5.1. Training Setup

Models were trained and tested with a batch size of 16 on a GPU cluster with 8 nodes, each with 8 NVIDIA RTX A5000 (24 GB on-board GPU memory), running Rocky Linux 8.5 and using Python 3.10 and PyTorch 1.13. For all models, we use early stopping with patience of 10 epochs to ensure convergence and avoid over-fitting.

### 5.2. Data

The refined dataset contains 12,000 images with and without cracks, along with the ground truth for each image. A random shuffling method was used to distribute the dataset between training, testing, and validation sets, with a ratio of 8:1:1. As a result, our dataset consists of 9,600 samples for the training, 1,200 samples for the testing, and 1,200 samples for the validation.

## 6. Experiments

### 6.1. Benchmarks

To assess the performance improvement of our model over traditional segmentation models, we compare it against FCN [27] and UNet [28]. Additionally, we include the DeepCrack2 model [10], a widely benchmarked crack detection model, as well as SegFormer [25] and HrSegNet-B64 [12], which represent SOTA models in semantic segmentation and crack segmentation, respectively. The performance of our model is assessed both quantitatively and qualitatively.

For all models, we used the Adam optimizer, set the initial learning rate to  $1.00e-04$ , and used a batch size of 16. Other hyperparameters are provided in Table 2.

Table 2: Hyperparameter settings of benchmarked models (LR indicates Learning Rate)

Model	LR Schedule	Pre-trained
Hybrid-Segmentor	ReduceLROnPlateau	ResNet (IMAGENET1K)
HrSegNet	ReduceLROnPlateau	None
DeepCrack2	None	None
SegFormer	PolynomialLR	None
UNet	None	None
FCN	None	VGG19 (IMAGENET1K)

### 6.2. Loss Functions

Experimentally, it has been demonstrated that class imbalance in datasets may be effectively addressed not only using a well designed architecture, but also using a well designed loss function [29, 30, 31]. To improve the robustness of our model, we evaluated the performance of various loss functions: Binary Cross Entropy (BCE) [32], Dice [30], the fusion of BCE and Dice [29], and Recall Cross Entropy (RecallCE) [31].

The BCE loss has been chosen for its ability to handle skewed pixel distributions effectively. In scenarios where one class significantly outweighs others, BCE loss computes an individual loss for each pixel to ensure proportional class contribution, mitigating any dataset bias. By treating pixels equally, the model is able to focus on accurately classifying minority classes, such as crack pixels, without being biased by dominant classes. BCE loss is described by the following equation:

$$BCE(y, \hat{y}) = -\frac{1}{N}(y_i \log(\hat{y}) + (1 - y_i) \log(1 - \hat{y}_i)) \quad (4)$$

where  $N$  is the total number of elements (pixels in the case of segmentation).  $y_i$  is the ground truth label (0 or 1) for the  $i$ -th element, and  $\hat{y}_i$  is the predicted probability for the  $i$ -th element.

Dice loss, which is equivalent to F1-score, is addressing the class imbalance focusing on capturing the overlap between predicted and ground truth masks, which helps address the challenge of minority class representation. By emphasizing object boundaries and assigning non-vanishing gradients to the minority class, Dice loss ensures accurate prediction and better learning

for smaller classes.

$$\text{Dice Loss} = 1 - \frac{2 \cdot \text{Intersection}}{\text{Union}} \quad (5)$$

Its ability to sensitively measure the similarity between prediction and ground truth makes it particularly useful for precise segmentation. It can be used alongside other losses such as BCE loss to keep a balance between handling class imbalance and capturing fine details [29]. Here, we used a combination of BCE and Dice losses as follows:

$$\text{BCE-DICE} = \lambda * \text{BCE loss} + (1 - \lambda) * \text{Dice loss} \quad (6)$$

where  $\lambda$  represents the weight (importance) attributed to the two loss functions and takes values between 0 and 1.

Previous methods attempt to improve standard cross-entropy loss in segmentation tasks by incorporating weighted factors. However, this approach can lead to issues such as reduced precision and increased false positive rate for minority classes. To address this problem, RecallCE loss is proposed as a hard-class mining solution. It reshapes the traditional cross-entropy loss by dynamically adjusting class-specific loss weights according to a real-time recall score, offering a more effective way to handle class imbalance and improve segmentation precision [31]. We evaluate the performance of our model by comparing the RecallCE loss with the other losses previously mentioned, to determine if it enhances our model’s effectiveness. The equation for RecallCE loss is as follows:

$$\text{RecallCE} = - \sum_{c=1}^C \sum_{n:y_i=c} (1 - R_{c,t}) \log(p_{n,t}) \quad (7)$$

where  $R_{c,t}$  represents the recall of class  $c$  during optimisation iteration  $t$ .

## 7. Evaluation

We carry out two prior studies to examine specific aspects of our model: (1) assessing the impact of individual encoder paths and (2) evaluating the performance of various loss functions. Initially, we aim to understand how distinctively each encoder extracts features. Then, we investigate which of the aforementioned individual loss functions and the combination of BCE and Dice losses (by assigning different weights) yields the best results in crack

segmentation. Once we determine the loss function providing the optimal performance, we compare our final model against SOTA crack segmentation models.

### 7.1. Encoder Paths

We conduct an experiment involving the training and testing of the two different encoders to assess their abilities in feature extraction. Specifically, we aim to determine whether convolutional layers perform well at extracting local features while transformers are adept at capturing global features. Each path was trained as an independent network by removing the influence of the other, and was compared against the fused network. An identical loss function was used for all networks for a fair comparison (BCE-DICE loss with  $\lambda = 0.5$ ).

The results presented in Table 3 indicate that the CNN path achieves a higher precision score than the transformer path, while the latter excels in terms of recall. This suggests that the transformer tends to produce more false positives, mistakenly predicting non-crack pixels as cracks. On the other hand, the CNN path tends to produce more false negatives, possibly misclassifying crack pixels as non-cracks. These results suggest that the transformer path captures broader areas as cracks, while the CNN path captures finer details. Combining the two paths into a fused model leverages the power of both and improves the accuracy and precision of crack segmentation, without significantly sacrificing recall. Fig. 4, shows example segmentations produced by each of the two encoders, further illustrating the differences in their performance.

### 7.2. Loss functions

We utilize various types of losses (BCE, Dice, and RecallCE) for addressing class imbalances and capturing fine-grained details. Our experiments

Table 3: Comparison and Performance Analysis of CNN and Transformer Paths

Model Name	Accuracy	Precision	Recall	F1 Score (Dice)	IOU score
<b>Hybrid-Segmentor (combined)</b>	<b>0.970</b>	<b>0.805</b>	<b>0.732</b>	<b>0.765</b>	<b>0.622</b>
CNN path	0.969	0.802	0.722	0.758	0.614
Transformer path	0.965	0.717	0.772	0.741	0.592

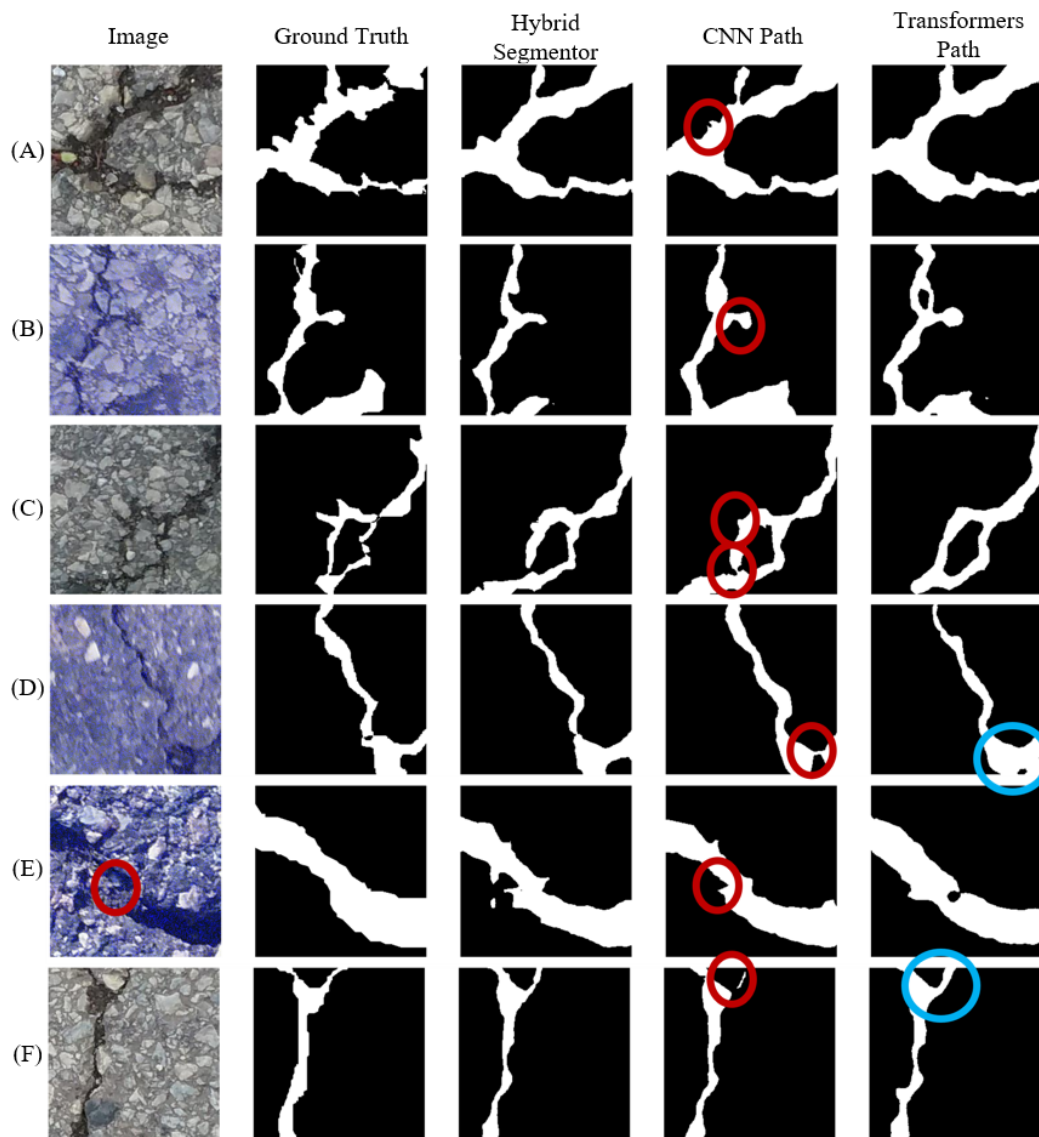


Figure 4: Hybrid model performance compared against CNN and transformer paths. The CNN path captures detailed contours (red circles), while the Transformer path gives an overall structure but with thicker predictions (blue circles).

Table 4: Performance of all combinations of loss functions

Loss Functions ( $\lambda$ )	Accuracy	Precision	Recall	F1 Score (Dice)	IOU score
DICE	0.970	0.807	0.727	0.763	0.620
BCE-DICE (0.1)	0.970	0.796	0.741	0.765	0.622
BCE-DICE (0.2)	<b>0.971</b>	0.804	0.744	<b>0.770</b>	<b>0.630</b>
BCE-DICE (0.3)	0.970	0.809	0.719	0.759	0.615
BCE-DICE (0.4)	0.970	0.809	0.720	0.760	0.616
BCE-DICE (0.5)	0.970	0.805	0.732	0.765	0.622
BCE-DICE (0.6)	0.970	0.805	0.736	0.767	0.625
BCE-DICE (0.7)	0.970	0.808	0.724	0.762	0.618
BCE-DICE (0.8)	0.969	<b>0.817</b>	0.700	0.752	0.605
BCE-DICE (0.9)	0.969	0.804	0.719	0.757	0.612
BCE	0.969	0.778	0.750	0.762	0.618
RecallCE	0.970	0.795	<b>0.746</b>	0.768	0.626

reveal that combining BCE and Dice losses provides a balance between recognizing dominant classes and accurately segmenting minority groups, resulting in a more effective model for imbalanced data than when using the loss functions individually (Table 4). We assess these aspects by varying the weights assigned to BCE and DICE loss functions. When BCE and DICE loss weights are roughly equal, the model generally performs better. A BCE-DICE loss with  $\lambda = 0.2$  outperforms other values in all metrics except for precision. Precision peaks at 0.817, but this trades off with recall, resulting in relatively lower performance in other metrics. Expectedly, RecallCE results in the highest recall score, as it penalizes the model heavily for false negatives while producing well-balanced results for the other metrics. However, this loss is behind BCE-DICE in terms of accuracy and precision, indicating that it may be less effective at addressing class imbalance. In summary, the BCE-DICE loss with  $\lambda = 0.2$  exhibits the best model performance, and was chosen as the loss function for our final model.

### 7.3. Comparison against SOTA models

We compare our best model using BCE-DICE loss ( $\lambda = 0.2$ ) to the benchmark models in our experiment. As demonstrated in Table 5, our model notably outperforms the other five models. Our model achieved an accuracy of 0.971, a precision of 0.804, a recall of 0.744, an F1-score of 0.770, and



Table 5: Performance of our crack segmentation model against state-of-the-art models

Model Name	Accuracy	Precision	Recall	F1 Score (Dice)	IOU score
FCN	0.968	0.802	0.702	0.746	0.598
UNet	0.968	0.789	0.720	0.750	0.603
DeepCrack2	0.968	0.788	0.704	0.741	0.592
SegFormer	0.965	0.750	0.719	0.730	0.580
HrSegNet	0.969	0.800	0.724	0.757	0.612
Hybrid-Segmentor	<b>0.971</b>	<b>0.804</b>	<b>0.744</b>	<b>0.770</b>	<b>0.630</b>

an IOU score of 0.630. These results demonstrate the model’s exceptional proficiency in crack segmentation tasks.

Qualitatively, our model exhibits significant improvements relative to existing models (Fig. 5). As shown by rows (A) and (C), our model handles crack discontinuity more accurately. Furthermore, in (B), our model excels at identifying vague cracks that other models fail to detect. When it comes to cracks on different types of surfaces, the proposed model works effectively regardless of the surface. While crack detection on brick surfaces is challenging due to the ambiguity between cracks and brick borders and resulting shadows, as shown in (D), our model is adept at handling such scenarios. On the other hand, models such as FCN incorrectly predict brick borders as cracks. Additionally, a challenge in crack detection involves identifying non-crack areas within cracked regions, which our model effectively addresses, as evident in (E) and (G). Example (H) demonstrates that our model works relatively well on blurred images. Furthermore, (F) demonstrates the superiority of our model in detecting intricate crack contours, in comparison to the other models that have significantly more false positives.

## 8. Limitations

Although our model outperforms other benchmarked models in performance, it still exhibits certain limitations. Two primary shortcomings of our model have been identified and presented in Fig. 6. Our model outperforms the other models in detecting thicker cracks within web-shaped crack patterns, except for UNet; however, it still faces challenges in identifying the thinner branches in these patterns. As illustrated in example images (A) to (D), while our model successfully detects the most prominent cracks, it

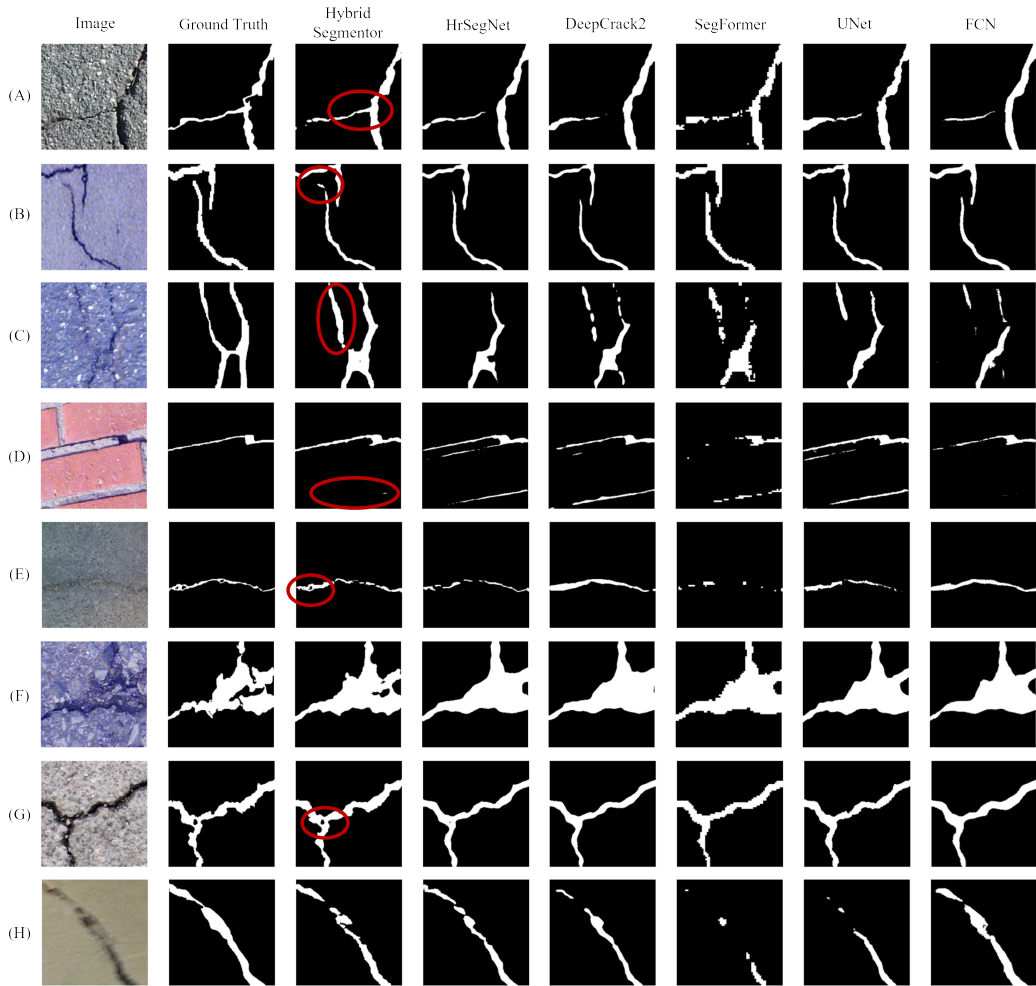


Figure 5: Example crack images segmented by our model and benchmarked models. The red ovals highlight the areas where our model outperforms other benchmarked models. In examples without red ovals, such as (F) and (H), our model demonstrates strong performance across overall structures.

struggles with extremely fine and delicate ones. This indicates an area where further improvement is possible.

Secondly, our model is sensitive to disruptions caused by distortions, such as occlusions and watermarks. (E) illustrates a situation where the watermark located within the crack is identified as a non-crack area. However, in (F), even with the presence of a watermark, our model fails to predict the cracks hidden by a translucent occlusion. Furthermore, (G) demonstrates an

issue where the model does not recognize letters on the road as part of the background. The variation in model performance may be attributed to the clear color contrast between the letters and the background, causing confusion for the model. It should be emphasized that all these challenges are common to all crack detection models. However, our model demonstrates better overall precision and elaboration in crack detection compared to others.

We believe that there is room for improvement to the model architecture for addressing these limitations. Additionally, techniques such as Generative Adversarial Networks (GANs) and meta-learning can be harnessed to generate synthetic data during the pre-processing phase to further deal with the lack of data and potential class imbalance issues. Furthermore, recognizing the increasing need for 3D crack image segmentation, the creation of high-quality 3D crack image datasets becomes imperative to advance this domain.

## 9. Conclusion

In this research, we have proposed a novel model for crack segmentation called Hybrid-Segmentor. This architecture incorporates two distinct encoder paths, namely the CNN path and the Transformer path. For the CNN path, we use the well-established ResNet-50 architecture[24], which is renowned for its ability to extract local features. Additionally, we introduce the concept of Overlapping Patch Embedding, Efficient Self-Attention, and Mix-FFN in the Transformer path, derived from the SegFormer [25] model. In combining two encoders, these additions optimize computational efficiency and model size, thereby soothing capacity problems. We further simplify the model with a relatively simpler decoder to minimize its size.

Through experimentation, Hybrid-Segmentor emerges as a SOTA, outperforming other renowned benchmark models. Our model effectively takes advantage of the two encoder paths, as proved by prior studies evaluating its performance in extracting local and global crack features. Based on the findings of previous studies, the BCE-DICE loss, weighted at 0.2 on the BCE loss, yields the best performance. In qualitative analysis, our model improves in addressing discontinuities, detecting small non-cracked areas within cracks, and recognizing cracks even in low-quality images and diverse surfaces. It is capable of capturing more details in crack contours than previous models.

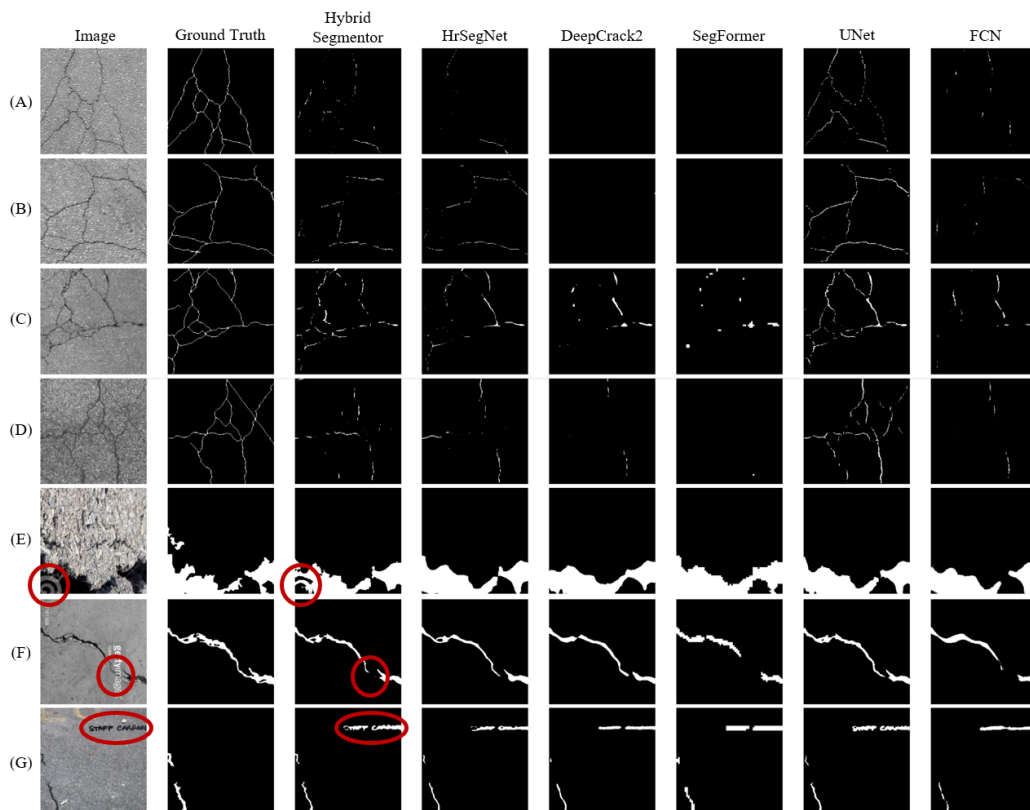


Figure 6: Examples of Hybrid-Segmentor’s limitations, including failure to detect thin or web-shaped objects and difficulties with occlusions.

Furthermore, our study introduces a data refinement methodology for combining publicly available datasets comprising 13 open-source crack datasets with refined ground truths. Since these datasets initially used diverse standards for creating ground truth, we merge and improve them to ensure equivalence, thereby increasing their reliability and precision. In addition, we employ a specific data augmentation approach in order to address the issue of class imbalance within our dataset. By extracting data containing cracks with more than 5000 pixels and augmenting them, we are able to incorporate these samples into our dataset. Our effort resulted in a dataset consisting of 12,000 crack images, each with its corresponding ground truth.

To enhance our crack detection model, we need to concentrate on enhancing the architecture to efficiently recognize thin, web-shaped cracks, and those that are hidden by occlusions. We could also explore the possibility

of using GANs and meta-learning to create synthetic data to overcome data scarcity, particularly in the development of 3D crack image segmentation datasets.

## 10. Acknowledgment

The research work of Dr. Alessandro Artusi and Dr. Xenios Milidonis has been partially funded from the European Union’s Horizon 2020 research and innovation programme under grant agreement No. 739578 and from the Government of the Republic of Cyprus through the Deputy Ministry of Research, Innovation and Digital Policy.

## References

- [1] X. Yang, H. Li, Y. Yu, X. Luo, T. Huang, X. Yang, Automatic pixel-level crack detection and measurement using fully convolutional network, *Computer-Aided Civil and Infrastructure Engineering* 33 (12) (2018) 1090–1109.
- [2] A. Zhang, K. Wang, Y. Fei, Y. Liu, C. Chen, G. Yang, J. Li, E. Yang, S. Qiu, Automated pixel-level pavement crack detection on 3d asphalt surfaces with a recurrent neural network: Automated pixel-level pavement crack detection on 3d asphalt surfaces using cracknet-r, *Computer-Aided Civil and Infrastructure Engineering* 34 (08 2018). doi:10.1111/mice.12409.
- [3] Y. Liu, J. Yao, X. Lu, R. Xie, L. Li, Deepcrack: A deep hierarchical feature learning architecture for crack segmentation, *Neurocomputing* 338 (2019) 139–153. doi:10.1016/j.neucom.2019.01.036.
- [4] J. Cheng, W. Xiong, W. Chen, Y. Gu, Y. Li, Pixel-level crack detection using u-net, in: *TENCON 2018 - 2018 IEEE Region 10 Conference, 2018*, pp. 0462–0466. doi:10.1109/TENCON.2018.8650059.
- [5] O. Oktay, J. Schlemper, L. L. Folgoc, M. Lee, M. Heinrich, K. Misawa, K. Mori, S. McDonagh, N. Y. Hammerla, B. Kainz, et al., Attention u-net: Learning where to look for the pancreas, *arXiv preprint arXiv:1804.03999* (2018).

- [6] J. König, M. D. Jenkins, M. Mannion, P. Barrie, G. Morison, Optimized deep encoder-decoder methods for crack segmentation, *Digital Signal Processing* 108 (2021) 102907.
- [7] D. Pal, P. B. Reddy, S. Roy, Attention uw-net: A fully connected model for automatic segmentation and annotation of chest x-ray, *Computers in Biology and Medicine* 150 (2022) 106083.
- [8] F. Panella, A. Lipani, J. Boehm, Semantic segmentation of cracks: Data challenges and architecture, *Automation in Construction* 135 (2022) 104110.
- [9] J. Deng, W. Dong, R. Socher, L.-J. Li, K. Li, L. Fei-Fei, Imagenet: A large-scale hierarchical image database, in: *2009 IEEE Conference on Computer Vision and Pattern Recognition*, 2009, pp. 248–255. doi:10.1109/CVPR.2009.5206848.
- [10] Q. Zou, Z. Zhang, Q. Li, X. Qi, Q. Wang, S. Wang, Deepcrack: Learning hierarchical convolutional features for crack detection, *IEEE Transactions on Image Processing* 28 (3) (2019) 1498–1512. doi:10.1109/TIP.2018.2878966.
- [11] V. Badrinarayanan, A. Kendall, R. Cipolla, Segnet: A deep convolutional encoder-decoder architecture for image segmentation, *IEEE transactions on pattern analysis and machine intelligence* 39 (12) (2017) 2481–2495.
- [12] Y. Li, R. Ma, H. Liu, G. Cheng, Real-time high-resolution neural network with semantic guidance for crack segmentation, *Automation in Construction* 156 (2023) 105112.
- [13] R. Amhaz, S. Chambon, J. Idier, V. Baltazart, Automatic crack detection on two-dimensional pavement images: An algorithm based on minimal path selection, *IEEE Transactions on Intelligent Transportation Systems* 17 (10) (2016) 2718–2729.
- [14] L. Zhang, F. Yang, Y. D. Zhang, Y. J. Zhu, Road crack detection using deep convolutional neural network, in: *2016 IEEE international conference on image processing (ICIP)*, IEEE, 2016, pp. 3708–3712.

- [15] Q. Zou, Z. Zhang, Q. Li, X. Qi, Q. Wang, S. Wang, Deepcrack: Learning hierarchical convolutional features for crack detection, *IEEE Transactions on Image Processing* 28 (3) (2019) 1498–1512.
- [16] Q. Zou, Y. Cao, Q. Li, Q. Mao, S. Wang, Cracktree: Automatic crack detection from pavement images, *Pattern Recognition Letters* 33 (3) (2012) 227–238.
- [17] M. Eisenbach, R. Stricker, D. Seichter, K. Amende, K. Debes, M. Sesselmann, D. Ebersbach, U. Stoeckert, H.-M. Gross, How to get pavement distress detection ready for deep learning? a systematic approach., in: *International Joint Conference on Neural Networks (IJCNN)*, 2017, pp. 2039–2047.
- [18] F. Yang, L. Zhang, S. Yu, D. Prokhorov, X. Mei, H. Ling, Feature pyramid and hierarchical boosting network for pavement crack detection, *IEEE Transactions on Intelligent Transportation Systems* (2019).
- [19] D. Dais, I. E. Bal, E. Smyrou, V. Sarhosis, Automatic crack classification and segmentation on masonry surfaces using convolutional neural networks and transfer learning, *Automation in Construction* 125 (2021) 103606. doi:10.1016/j.autcon.2021.103606.  
URL <https://linkinghub.elsevier.com/retrieve/pii/S0926580521000571>
- [20] Y. Shi, L. Cui, Z. Qi, F. Meng, Z. Chen, Automatic road crack detection using random structured forests, *IEEE Transactions on Intelligent Transportation Systems* 17 (12) (2016) 3434–3445.
- [21] L. Cui, Z. Qi, Z. Chen, F. Meng, Y. Shi, Pavement distress detection using random decision forests, in: *International Conference on Data Science*, Springer, 2015, pp. 95–102.
- [22] M. Maguire, S. Dorafshan, R. J. Thomas, Sdnet2018: A concrete crack image dataset for machine learning applications (2018).
- [23] S. Kulkarni, S. Singh, D. Balakrishnan, S. Sharma, S. Devunuri, S. C. R. Korlapati, Crackseg9k: A collection and benchmark for crack segmentation datasets and frameworks (2022). arXiv:2208.13054.

- [24] K. He, X. Zhang, S. Ren, J. Sun, Deep residual learning for image recognition, in: Proceedings of the IEEE conference on computer vision and pattern recognition, 2016, pp. 770–778.
- [25] E. Xie, W. Wang, Z. Yu, A. Anandkumar, J. M. Alvarez, P. Luo, Segformer: Simple and efficient design for semantic segmentation with transformers, *Advances in Neural Information Processing Systems* 34 (2021) 12077–12090.
- [26] A. Dosovitskiy, L. Beyer, A. Kolesnikov, D. Weissenborn, X. Zhai, T. Unterthiner, M. Dehghani, M. Minderer, G. Heigold, S. Gelly, et al., An image is worth 16x16 words: Transformers for image recognition at scale, *arXiv preprint arXiv:2010.11929* (2020).
- [27] J. Long, E. Shelhamer, T. Darrell, Fully convolutional networks for semantic segmentation, in: Proceedings of the IEEE conference on computer vision and pattern recognition, 2015, pp. 3431–3440.
- [28] O. Ronneberger, P. Fischer, T. Brox, U-net: Convolutional networks for biomedical image segmentation, in: *Medical Image Computing and Computer-Assisted Intervention–MICCAI 2015: 18th International Conference, Munich, Germany, October 5-9, 2015, Proceedings, Part III* 18, Springer, 2015, pp. 234–241.
- [29] Q. D. Nguyen, H.-T. Thai, Crack segmentation of imbalanced data: The role of loss functions, *Engineering Structures* 297 (2023) 116988. doi:<https://doi.org/10.1016/j.engstruct.2023.116988>. URL <https://www.sciencedirect.com/science/article/pii/S0141029623014037>
- [30] C. H. Sudre, W. Li, T. Vercauteren, S. Ourselin, M. Jorge Cardoso, Generalised dice overlap as a deep learning loss function for highly unbalanced segmentations, in: *Deep Learning in Medical Image Analysis and Multimodal Learning for Clinical Decision Support: Third International Workshop, DLMIA 2017, and 7th International Workshop, ML-CDS 2017, Held in Conjunction with MICCAI 2017, Québec City, QC, Canada, September 14, Proceedings 3*, Springer, 2017, pp. 240–248.
- [31] J. Tian, N. C. Mithun, Z. Seymour, H. Chiu, Z. Kira, Striking the right balance: Recall loss for semantic segmentation, *CoRR* abs/2106.14917



(2021). [arXiv:2106.14917](https://arxiv.org/abs/2106.14917).

URL <https://arxiv.org/abs/2106.14917>

- [32] M. Yi-de, L. Qing, Q. Zhi-bai, Automated image segmentation using improved pcnn model based on cross-entropy, in: Proceedings of 2004 International Symposium on Intelligent Multimedia, Video and Speech Processing, 2004., 2004, pp. 743–746. doi:10.1109/ISIMP.2004.1434171.